Supporting Information

SI Material and Methods

Microsomal fractionation. Liquid N2 frozen leaf tissue (about 600mg) was ground to fine powder with a pestle and mortar and 2mL ice cold sucrose buffer (20mM Tris (pH 8), 0.33M sucrose, 1mM EDTA, 5mM DTT and 1x Sigma Plant Protease Inhibitors) was added. Samples were filtered with miracloth filter paper and centrifuged in a microcentrifuge at 2,000 x g for 5 minutes at 4°C to remove debris. 200µl of supernatant was taken as the total lysate fraction (T). The rest of the lysate was then spun at 4°C at 20,000 x g for 60 minutes. 200µl of the resulting supernatant was used as the soluble fraction (S), the membrane pellet was resuspended in 600µl of ice cold sucrose buffer to yield the microsomal fraction (M).

Confocal Microscopy. Leaf discs (7 mm diameter) of 4-5 week old N. benthamiana leaves were collected 24 hours post Agro-infiltration (as described above). The abaxial side of leaves was imaged using a C-Apochromat 40X/NA1.2 water immersion lens on a Zeiss LSM710 confocal laser-scanning microscope. Images were taken with standardized excitation intensities and photomultiplier gains. XFP-fluorescence was imaged using an Argon/2 laser and the PMT (photomultiplier tube detector) to collect emissions. Excitation wavelength/emission bandwidth were set at 514/519-560 nm for eYFP and 561/580-630 nm for tRFP. Confocal images were edited with ZEN 2009 software and Adobe Photoshop CS5. Fluorescence intensity for the rBiFC experiment was measured with the co-localization function in the ZEN 2009 software and data was analyzed with Microsoft Excel 2010.

Generation of expression plasmids. Gateway-compatible Entry clones and Destination clones were generated by Topo, BP and LR cloning (Invitrogen). Site-directed mutants were generated with the QuickChange Lightning Site-Directed-mutagenesis Kit (www.agilent.com/). Oligonucleotides used for cloning were synthesized by eurofins mwg operon (www.eurofinsgenomics.com). RPM1 is C-terminally and RIN4 is N-terminally epitope tagged throughout the paper. Agrobacteria - CaMV 35S-promoter expression plasmids included: pGWB614 (3xHA, C-terminal), pGWB617 (4xMYC, C-terminal), pGWB641 (eYFP, C-terminal), pGWB661 (tRFP, N-terminal). The RPM1 native promoter::RPM1-myc or -eYFP

complementation constructs were generated by cloning a 1034bp long promoter fragment in front of the gateway cassette in pGWB616 and pGWB640, respectively. Sequences and maps of RPM1-promoter containing vectors are available at the Dangl laboratory website: http://labs.bio.unc.edu/dangl/Resources/Plasmid_Sequences/plasmid_seqs_index.htm.

The RPM1 CC-4 fragment was cloned into the previously published pMDC7 plasmid bearing an estradiol inducible promoter upstream of the gateway cassette followed by a YFP or CFP tag (1). For the BiFC experiments of RIN4 and RPM1 their coding sequences were Gateway cloned into the pBiFCt2in1 NC vector described in (2). The CC-2 and CC-2^{EEE} coding sequence were Gateway cloned into the pBAT-TLC and pBAT-TLN plasmids described in (3).

Bacterial strains and growth conditions. *Escherichia coli* Top10 and *Agrobacterium tumefaciens* strain GV3101/pMP90 were grown in LB media and 37°C and 28°C, respectively. *Pseudomonas syringae* strains were grown at 28°C in King's B media at 28°C. *E. coli* antibiotic concentrations used (in μg/mL) were: Ampicillin 100, Kanamycin 30, Gentamycin 25 and Spectinomycin 50. *Agrobacterium* antibiotic concentrations used (in μg/mL) were: Gentamycin 50, Kanamycin 100, Rifampicin 100, Spectinomycin 100. *Pseudomonas* antibiotic concentrations used (in μg/mL) were: Kanamycin 30, Rifampicin 50.

Bacterial assays and conductivity measurements. *Pseudomonas syringae* bacterial growth assays were performed as described (4). Briefly, *Pto* DC3000 was grown overnight and washed in 10mM $MgCl_2$, resuspended to OD_{600}=0.0002. These cultures were hand-injected with needleless syringes into 4-5 week-old Arabidopsis rosette leaves between 10 am and noon and phenotyped 6-12hr after infiltration for cell-death symptoms. Leaves were cored (#4 cork borer), ground and dilution plated to assess recovered colony-forming units at 2hr and 3 days post-infiltration. Each experiment contained six biological replicates per genotype and statistical significance was assessed using a one-way ANOVA and post-hoc Tukey's HSD ($p \leq 0.05$) (PRISM8.0). To measure conductivity, four leaf discs were collected with a #4 corer from 4 independent plants infiltrated 2 hours earlier. Leaf disks were added to clear tubes with 6ml of distilled water at room temperature under continuous light (three replicates per sample). Changes in water conductivity were measured at the indicated time points with an Orion Model 130. *Agrobacterium*

(GV3101/pMP90)-mediated transient expression assays were performed with 5-6 week-old *N. benthamiana* plants. Agrobacteria cultures were grown overnight in liquid medium, re-suspended in 10mM $MgCl_2$ amended with 10mM MES pH5.6 and 150μM acetosyringone. *Agrobacterium* carrying indicated constructs were injected on the abaxial site of leaves at an OD_{600} of 0.2 for RPM1 and derivatives, 0.2 for RIN4 and derivatives, and 0.2 for all RPM1 fragments. All infiltrations additionally included *Agrobacterium* carrying the viral silencing suppressor gene *P19* at and OD_{600} of 0.1.

RNA isolation and RT-PCR. Total RNA for RT-PCR analysis was extracted using the RNeasy Plant Mini Kit (Qiagen) and on-column DNA digestion with RNase-Free DNase Set (Qiagen) according to the manufacturer's protocol.

Structural modeling of RPM1. The protein sequence alignment between the RPM1 CC domain (aa1-120) and the Sr33 CC domain (aa1-120) was generated using the MUSCLE (Multiple Sequence Comparison by Log-Expectation) alignment tool (5). Then the protein sequence of the RPM1 CC domain (aa1-120) was submitted to the online server I-TASSER (6–8) using both the sequence alignment and the NMR structure of the Sr33 CC domain (PDB: 2NCG) as a template for structural modeling. The top model with a C-score of 0.45 and an estimated TM-score of 0.77±0.10 was selected for further analysis. Secondary structure prediction for *Fig. S1* and *Fig. S6A* was done by submitting the following RPM1 protein sequences, CC (aa1-155), NB-ARC (aa156-535) and LRR (aa536-926), to the JPred4 server (9) www.compbio.dundee.ac.uk/jpred/index.html).

Amino acid alignments. RPM1 (aa1-165), Sr33 (aa1-160), MLA10 (aa1-160) and Rx (aa1-164) CC domain sequences were aligned using the Clustal W alignment function in the CLC Main Workbench 7.7.3 software from QIAGEN. Alignment of Arabidopsis RPM1 and orthologues of other plant species was done with the Phytozome 10 online database (https://phytozome.jgi.doe.gov/pz/portal.html) and Clustal W function in the CLC Main Workbench 7.7.3 software. Full-length RPM1 protein sequence was used to identify BLASTp hits in other plant genomes (*Mtr, Medicago trunactula; Vvi, Vitis vinifera; Stu, Solanum tuberosum; Sly, Solanum lycopersicum; Esa, Eutrema salsugineum; Bst, Brachypodium stacei; Aly,*

Arabidopsis lyrata; Lus, Linum usitatissimum; Mes, Manihot esculante; Tca, Theobroma cacao; Ppe, Prunus persicus; Rco, Ricinus communis; Mdo, Malus domesticus; Fve, Fragaria vesca). The top hit in each proteome was downloaded and used for Clustal W alignment. Amino acids 1-174 (RPM1) are shown in the alignment.

Supplementary Fig. legends

Fig. S1. Secondary structure prediction of full-length RPM1.

Fig. S2. Immune signaling is induced by activated full-length RPM1 only. **(*A*)** Schematic overview of full-length RPM1 and RPM1 fragments/domains used throughout this work. Fragment end- and start points were chosen based on secondary structure predictions and sequence comparisons with other plant NLR proteins. Numbers indicate amino acid start- and endpoints of indicated domains and fragments. **(*B*)** Lack of cell death induction by myc-epitope tagged RPM1 fragments and full-length RPM1 transiently expressed in *N. benthamiana*. MHD mutant RPM1^{D505V} was used as a positive control. **(*C*)** Lack of cell death induction in *N. benthamiana* by myc-epitope tagged RPM1 fragments transiently expressed alone (left column), together with RIN4^{T166D} (middle column), RIN4 and dexamethasone inducible AvrRpm1-HA (right column). NB-ARC containing fragments/domains with the MHD motif mutation D505V and infiltration controls are shown in the right column, bottom. Images shown are representative of at least three biological replicates with at least 5 technical repeats each. Red boxes indicate positive controls for HR: full-length RPM1 with RIN4^{T166D} and full-length RPM1 together with RIN4 and AvrRpm1. **(*D*)** Epitope-tag does not influence lack of HR induction in transient expression in *N.benthamiana* by individual RPM1 fragments. Leaf images show representative results of expression of indicated non-tagged fragments individually; MHD motif mutant RPM1^{D505V} was used as a positive control for HR. DNA-gel pictures demonstrate transcription of indicated fragments *in planta*. M, DNA-ladder; Crtl, positive control; EV, empty vector infiltration control; +RT and –RT, plus and minus reverse transcriptase, respectively. **(*E*)** Expression of myc-tagged RPM1 fragments and full-length protein, T7-tagged wild type and phosphomimetic RIN4 and HA-tagged AvrRpm1 from experiment shown in A. Proteins were extracted from transiently transformed *N. benthamiana* leaves 24 hours after infiltration (and 6 hours post induction in the case of dexamethasone inducible AvrRpm1-HA) and analyzed by immunoblotting with anti-myc,

anti-T7 and anti-HA antibodies. Ponceau staining (PS) of the RuBisCO large subunit is a protein loading control. **(*F*)** Stable transgenic expression of YFP-HA tagged CC-4 fragment under the control of the estradiol inducible promoter in *pRIN4::T7-RIN4 rpm1-3 rps2-102c rin4* (*r1r2r4*) mutant Arabidopsis does not complement lack of AvrRpm1 recognition. Macroscopic HR in leaves of indicated genotypes 8 hours post infiltration of *Pto* DC3000(*avrRpm1*) and 24 hours post estradiol induction (upper panel). Immunoblot with anti-HA antibodies shows expression of 8 individual T3 lines expressing the YFP-HA tagged CC-4 fragment. Three plants each were pooled for protein extraction 6 hours after estradiol induction. Ponceau staining (PS) of the RuBisCO large subunit is a protein loading control. **(*G*)** Stable transgenic expression of YFP-HA tagged CC-2 and CC-NB-ARC fragments under the control of the 35S promoter in *rpm1-3* mutant Arabidopsis does not complement lack of AvrRpm1 recognition. Quantitative measurement of cell death (ion-leakage/conductivity) induced by activation of wild type RPM1 and indicated RPM1 fragments upon infiltration of *Pto* DC3000(*avrRpm1*) (left). Immunoblotting with anti-myc, anti-HA and anti-ATPase (for protein loading control) antibodies of indicated transgenic expressed proteins are shown (right).

Fig. S3. Localization of RPM1 fragments and domains. Cell fractionation experiments show strong membrane localization of RPM1 CC-2, NB-ARC and the CC-NB-ARC fragments. myc-tagged 35S-driven RPM1 fragments were infiltrated into *N. benthamiana* leaves and tissue was harvested 48 hours post infiltration for cell-fractionation and western-blotting with anti-myc (RPM1), anti-APX (cytosol) and anti-H3 (Histone 3, membrane) antibodies. Ponceau S (PS) staining served as a protein loading control and an additional marker for the cytosolic fraction. T, total extract; S, soluble; M, microsomal fraction. M(3X) indicates 3 times enrichment relative to T or S.

Fig. S4. *In planta* RPM1-RIN4 interaction is primarily mediated through the NB-ARC and LRR domains. **(*A*)** shows the interaction of the CC-1, NB-ARC, LRR and NB-ARC-LRR with wild type RIN4 and **(*B*)** the interaction of the NB-ARC, LRR and NB-ARC-LRR with RIN4^{T166D} transiently expressed in *N. benthamiana*. **(*C-F*)** Interaction analysis of transiently expressed CC-1 (*C*), CC-2 (*D*), NB-ARC (*E*) and LRR (*F*) domains with RIN4, RIN4^{T166A}, RIN4^{T166D} and RIN4^{F169A} by co-immunoprecipitation. RPM1 fragments were 35S promoter-driven and C-terminally myc-tagged, and N-terminal T7-tagged genomic

RIN4 was expressed from its native promoter. Lysates were immunoprecipitated with anti-myc beads and then immunoblotted for both anti-myc and anti-T7 to assess input, immunoprecipitation and co-immunoprecipitation. Protein loading in input was assessed by Ponceau staining (PS). The $RIN4^{F169A}$ mutant was used as a negative control for RPM1 fragment – RIN4 interaction. Note: bands present on the right in the anti-myc blot of the coIP fraction in (*C*) are non-specific, and the control experiment in (*D*) is from the same experiment as presented in (*C*), therefore the same control – RIN4 alleles w/o CC – is shown.

Fig. S5. RPM1 self-association and membrane localization is P-loop dependent. **(*A*)** Complementation of the *rpm1* mutant by the *pRPM1::RPM1-GFP* construct used to generate a double transgenic line. Table shows segregation of HR positive plants of one selected heterozygous T2 line. 44 plants were infiltrated with *Pto* DC3000(*avrRpm1*) (OD_{600}=0.1) and HR was scored 8 hours post infiltration. Bar-graph shows bacterial growth assay of indicated genotypes infiltrated with *Pto* DC3000(*avrRpm1*) (OD_{600}=0.0002) to assess complementation of growth restriction by *pRPM1::RPM1-GFP* in *rpm1-3*. WT, Col-0; *rpm1, rpm1-3; rpm1 pRPM1::RPM1-GFP*. **(*B*)** Self-association of RPM1-myc and RPM1-GFP in Arabidopsis. Stable transgenic expression in Arabidopsis was under the control of the *RPM1* promoter. Proteins were immunoprecipitated with anti-myc magnetic beads and then immunoblotted for both anti-myc and anti-GFP to assess input, immunoprecipitation and co-immunoprecipitation. **(*C*)** Cell fractionation analysis of wild type and P-loop alleles indicates decreased membrane localization of P-loop mutants. Indicated myc-tagged 35S-driven RPM1 constructs were infiltrated into *N. benthamiana* leaves and tissue was harvested for cell-fractionation and immunoblotting with anti-myc (RPM1) and anti-H^+ATPase (membrane) antibodies. Ponceau S (PS) staining is a protein loading control and marker for cytosolic fraction. T, total extract; S, soluble; M, microsomal fraction. M(3X) indicates 3 times enrichment relative to T or S.

Fig. S6. Lanthanum ($LaCl_3$)-treatment does not affect RPM1-mediated disease resistance. **(*A*)** RPM1 protein accumulation upon $LaCl_3$-treatment. Disappearance of activated RPM1 was blocked by infiltration of 2mM $LaCl_3$ 30 minutes before dexamethasone (20uM) spraying to induce expression of the effector AvrRpm1-HA. AvrRpm1-inducing RIN4 phosphorylation was monitored with ~1 kDalton mobility shift by

immunoblotting with anti-RIN4 (asterisk). AvrRpm1 expression was shown in immunoblot with anti-HA. Rubisco represents the protein loading control. **(*B*)** RPM1-mediated disease resistance in response to *Pto* DC3000(*avrRpm1*) in the presence of $LaCl_3$. 1.5mM $LaCl_3$ was added to the bacterial suspension ($1x10^5$ cfu/mL) and hand-infiltrated into leaves of Arabidopsis Col-0 plants. Bacterial growth of *Pto* DC3000(*avrRpm1*) and *Pto* DC3000(*EV*) was monitored at Day 0 and Day 3 with repeated application of 2mM $LaCl_3$ at 24 hour intervals. Student's *t*-test ($p < 0.01$) of bacterial growth in Day 0 or Day 3 was performed, respectively, and significance is indicated by letters in the bars. Error bars represent 2 x SE. **(*C*)** No effect of $LaCl_3$ on bacterial growth. The same amount of bacteria as used above ($1x10^5$ cfu/mL) was cultured in King's B media for 3 hours with and without 2mM $LaCl_3$. Statistical analysis was performed as in (*B*). Error bars represent 2 x SE and significance is indicated by letters in the bars.

Fig. S7. Mutations in hydrophobic and conserved residues of the CC domain affect RPM1 function. **(*A*)** Protein sequence alignment and secondary structure prediction of full-length CC domain of Arabidopsis RPM1 and RPM1 orthologues. Red bars represent position of predicted alpha-helices for RPM1 CC domain. Positions of residues mutated and analyzed throughout this work are indicated and their conservation is highlighted by a red (hydrophobic residues) or blue (conserved residues) box. Transcript names are shown for each RPM1 orthologue in the specific plant species. Mtr, *Medicago truncatula*; Vvi, *Vites vinifera*; Stu, *Solanum tuberosum*; Sly, *Solanum lycopersicum*; Esa, *Eutrema salsugineum*; Bst, *Boechera stricta*; Aly, *Arabidopsis lyrata*; Ath, *Arabidopsis thaliana*; Lus, *Linum usitatissimun*; Mes, *Manihot esculenta*; Tca, *Theobroma cacao*; Ppe, *Prunus persicus*; Rco, *Ricinus communis*; Mdo, *Malus domesticus*; Fve, *Fragaria vesca*. **(*B-E*)** HR phenotypes induced by transient expression of the 35S promoter-driven CC domain mutants $RPM1^{I31E}$, $RPM1^{M34E}$, $RPM1^{M41E}$, $RPM1^{S43F}$ and $RPM1^{P105S}$ alone (*B*), together with RIN4 (*C*), phosphomimetic $RIN4^{T166D}$ (*D*) or RIN4 and dexamethasone inducible AvrRpm1 (*E*). Wild type RPM1 and MHD motif mutant $RPM1^{D505V}$ were used as controls. Images were taken 2 days post infiltration. Note that the mutations in the three hydrophobic residues I31, M34 and M34 as well as in P105 did not completely abolish RPM1 function when transiently over-expressed from the 35S promoter. **(*F*)** Loss of full activity of the $RPM1^{I31/M34/M41E}$ (EEE) triple mutant in the transient reconstruction assay in *N. benthamiana*. Left side of the leaf shows the control phenotypes with

infiltrations of wild type RPM1 and the RPM1$^{I31/M34/M41E}$ (EEE) triple mutant alone and the right side of the leaf shows the experiment infiltrations with the triple mutant in co-expression with wild type RIN4 (upper right side), phosphomimetic RIN4^{T166D} (middle right side) and with wild type RIIN4 and dexamethasone inducible AvrRpm1 (lower right side). **(*G*)** HR phenotypes induced by *in cis* double mutants RPM1$^{I31E/D505V}$, RPM1$^{M34E/D505V}$, RPM1$^{M41E/D505V}$, RPM1$^{S43F/D505V}$ and RPM1$^{P105S/D505V}$. RPM1^{D505V} single mutant was used as a control for HR induction. Note that only the S43F mutation completely blocks RPM1^{D505V} auto-activity. **(*H*)** Complete block of RPM1^{D505V} auto-activity by RPM1$^{I31/M34/M41E}$ in the RPM1$^{I31/M34/M41E/D505V}$ *cis* quadruple mutant. All mutant RPM1 proteins in (*B-H*) were expressed from the 35S promoter. RIN4 and phosphomimetic RIN4^{T166D} were expressed from the RIN4 promoter. Images were taken 2 days post infiltration. **(*I, J*)** Expression of wild type and mutant RPM1 proteins shown in Fig. 3 *B* and *C*. Immunoblotting with anti-GFP and anti-T7 antibodies demonstrates accumulation of pRPM1::RPM1-eYFP (wild type and mutants) and phosphomimetic pRIN4::T7-RIN4^{T166D} proteins transiently expressed in *N. benthamiana*.

Fig. S8. Structural modelling of the RPM1 CC domain onto the Sr33 CC domain structure. **(*A*)** NMR structure of Sr33 CC domain (aa 3-120; PDB: 2NCG) as published by Casey et al. (10). N and C-termini are indicated. **(*B*)** Modelled structure of RPM1 CC domain (aa 1-120) indicates a very similar four-helical bundle conformation. Mutations used in this study are highlighted: hydrophobic residues I31, M34 and M41 in purple, conserved residues S43 and P105 in orange. The conserved EDVID motif (in RPM1 it is EDILD) is highlighted in blue. N and C-termini are indicated. **(*C, D*)** Overlay of the Sr33 (cyan) and RPM1 (green) CC domain structures, presented in a side view (*C*) and in a side view turned about 50 degrees to the viewer (*D*). Mutations in (*D*) are highlighted as in (*B*).

Fig. S9. RPM1-RIN4 interaction is dependent on the P-loop and the CC domain hydrophobic core. **(*A*)** The indicated myc-tagged 35S-driven RPM1 constructs were infiltrated into *N. benthamiana* leaves and tissue was harvested for cell-fractionation and western-blotting with anti-myc (RPM1), anti-H+ATPase (membrane) antibodies. Ponceau S (PS) staining served as protein loading control and marker for the cytosolic fraction. **(*B*)** Co-localization of RPM1$^{I31/M34/M41E}$-eYFP (pR1::EEE-eYFP) and tRFP-T7-RIN4 at

the plasma membrane in *N. benthamiana* leaf-epidermal cells. pRPM1::RPM1$^{I31/M34/M41E}$-eYFP and 35S::tRFP-T7-RIN4 were co-infiltrated into 5 week old *N. benthamiana* leaves at and OD_{600} of 0.4 and 0.2, respectively and images were taken 48 hours post infiltration with a Leica LSM710 DUO confocal microscope. **(*C*)** Cell fractionation analysis of RPM1$^{I31/M34/M41E}$ demonstrates membrane localization. Indicated myc-tagged 35S-driven RPM1$^{I31/M34/M41E}$ and T7-RIN4 were infiltrated into *N. benthamiana* leaves and tissue was harvested for cell-fractionation and immunoblotting with anti-myc (RPM1) and anti-T7 (membrane) antibodies. Ponceau S (PS) staining served as protein loading control and marker for cytosolic fraction. T, total extract; S, soluble; M, microsomal fraction. M(3X) indicates 3 times enrichment relative to T or S. **(*D*)** Interaction of RPM1 with wild type RIN4 is P-loop dependent and also abolished by the triple CC domain mutation (EEE). T7-RIN4 was co-expressed with wild type or mutant myc-epitope tagged RPM1 in *N. benthamiana*. Proteins were immunoprecipitated with anti-myc magnetic beads and immunoblotted for both anti-myc and anti-T7 to assess input, immunoprecipitation and co-immunoprecipitation. **(*E*)** Interaction of phosphomimetic RIN4^{T166D} with RPM1 is strongly reduced by mutations in hydrophobic residues of the CC domain and mutation in the P-loop. Samples were processed as described in *D*. RPM1 and its derivatives were expressed from the 35S promoter, RIN4 and RIN4^{T166D} from its native promoter. Experiments were repeated two times with similar results. **(*F*)** Expression analysis of RPM1 and RIN4 derivatives shown in the BiFC experiment in Fig. 5H and I. Immunoblotting with anti-HA and anti-myc antibodies demonstrates accumulation of RPM1-HA-nYFP and cYFP-myc-RIN4. **(*G*)** Forced membrane-tethering of RPM1^{G205E} or RPM1$^{G205E/D505V}$ does not “rescue” loss of RIN4 interaction. Samples were processed as described in *D*. CBL-tagged RPM1 and its derivatives were expressed from the 35S promoter, RIN4 from its native promoter.

Fig. S10. CC-2 dimerization is blocked by mutations in hydrophobic residues. **(*A*)** Bimolecular fluorescence complementation (BiFC) by self-association of 35S promoter driven CC-2-cYFP, CC-2-nYFP, but not by CC-2^{EEE}-cYFP, CC-2^{EEE}-nYFP. Expression constructs were transiently expressed in *N. benthamiana* after infiltration of *Agrobacterium* containing indicated constructs at an OD_{600}=0.3. Images were taken 40 hours post infiltration. **(*B*)** Expression analysis of CC-2 and CC-2^{EEE} of the BiFC

experiment in (*A*). Immunoblotting with anti-HA and anti-myc antibodies demonstrates accumulation of CC-2-HA-cYFP, CC-2-myc-nYFP and CC-2^{EEE}-HA-cYFP, CC-2^{EEE}-myc-nYFP.

Fig. S11. Protein sequence alignment of Arabidopsis CNLs showing the conservation of Gly174. Sequences between amino acid 159-223 of RPM1 and other CNLs were aligned using the CLC Main Workbench MUSCLE alignment function. Color code indicates conservation of amino acids from low (blue) to high (red). Conserved Glycine residue and the P-loop are marked with a red arrow and a curly bracket, respectively. RPM1 sequence is highlighted by a green arrow.

References

1. Curtis MD, Grossniklaus U (2003) A gateway cloning vector set for high-throughput functional analysis of genes in planta. *Plant Physiol* 133(2):462–469.
2. Grefen C, Blatt MR (2012) A 2in1 cloning system enables ratiometric bimolecular fluorescence complementation (rBiFC). *BioTechniques* 53(5):311–314.
3. Urano D, et al. (2012) Endocytosis of the seven-transmembrane RGS1 protein activates G-protein-coupled signalling in Arabidopsis. *Nat Cell Biol* 14(10):1079–1088.
4. Morel JB, Dangl JL (1999) Suppressors of the arabidopsis lsd5 cell death mutation identify genes involved in regulating disease resistance responses. *Genetics* 151(1):305–319.
5. Edgar RC (2004) MUSCLE: multiple sequence alignment with high accuracy and high throughput. *Nucleic Acids Res* 32(5):1792–1797.
6. Zhang Y (2008) I-TASSER server for protein 3D structure prediction. *BMC Bioinformatics* 9:40.
7. Roy A, Kucukural A, Zhang Y (2010) I-TASSER: a unified platform for automated protein structure and function prediction. *Nat Protoc* 5(4):725–738.
8. Yang J, et al. (2015) The I-TASSER Suite: protein structure and function prediction. *Nat Methods* 12(1):7–8.
9. Drozdetskiy A, Cole C, Procter J, Barton GJ (2015) JPred4: a protein secondary structure prediction server. *Nucleic Acids Res* 43(W1):W389–94.
10. Casey LW, et al. (2016) The CC domain structure from the wheat stem rust resistance protein Sr33 challenges paradigms for dimerization in plant NLR proteins. *Proc Natl Acad Sci U S A*.

Fig. S1

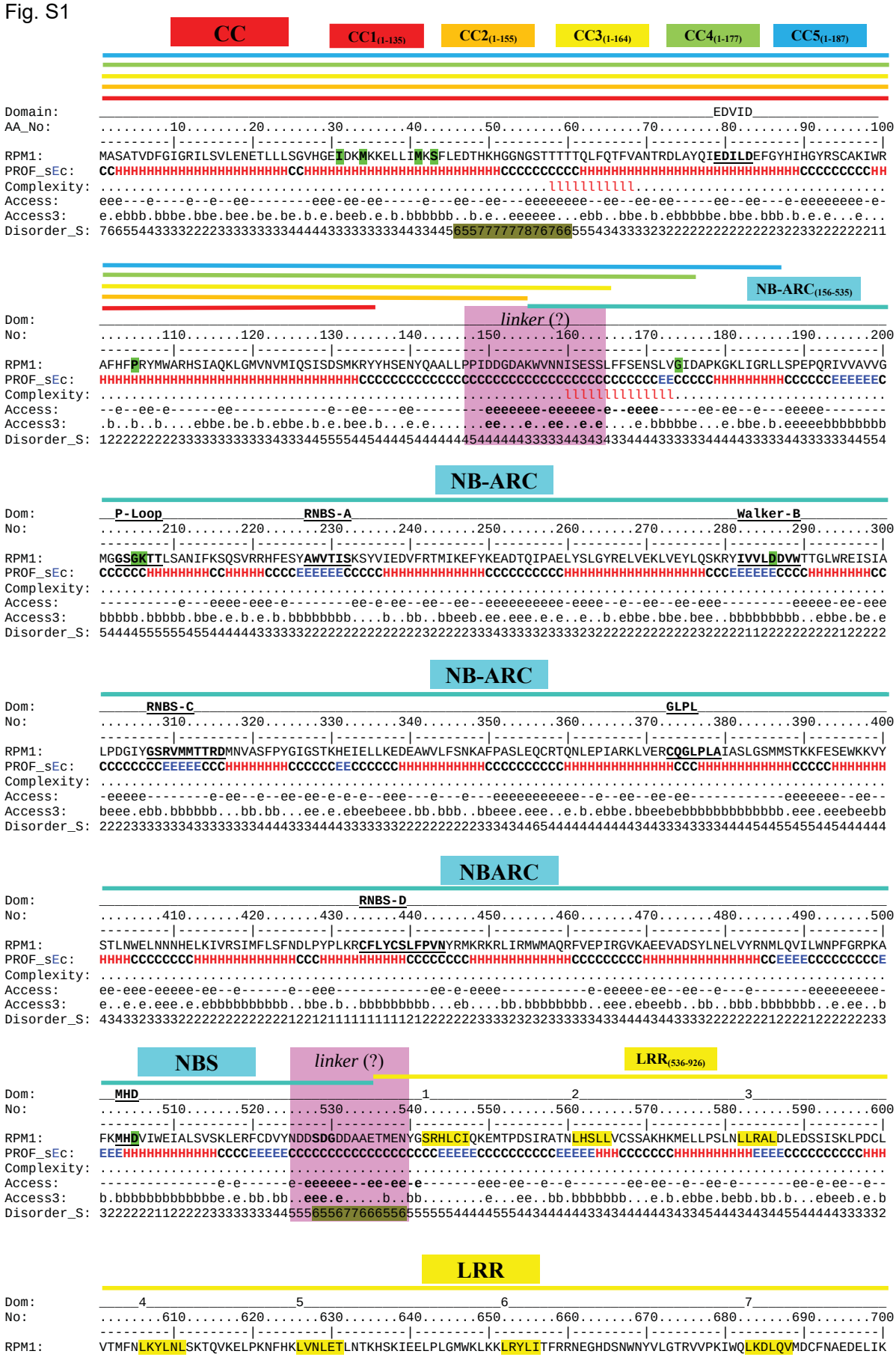
CC
CC1(1-135)
CC2(1-155)
CC3(1-164)
CC4(1-177)
CC5(1-187)
NB-ARC(156-535)
linker (?)
NB-ARC
P-Loop
RNBS-A
Walker-B
NB-ARC
RNBS-C
GLPL
NBARC
RNBS-D
NBS
linker (?)
LRR(536-926)
MHD
1
2
3
LRR
4
5
6
7

```
PROF_sEc:   HHHHHHHHHHCCCCCCCCCHHHHHHHHHHHHCCCCCCCCCCCCCHHHHHHHHHHHHHHHCCCCCCCCCCCCCCCCCCCCHHHHCCCCCHHHHCCCCCCCCCC
Complexity: ..........................................................................................................
Access:     ee---------ee-e-ee--ee-ee-ee----e-ee-e-ee--ee-ee-ee-------e-ee-eeee-e---e-e--ee-ee-ee-ee-e--e-eee--e
Access3:    b.bbbbbbb.b.e.e.eebbe.bbebb.b.bb.be..ebeeb.e.b.eb..b.bbbbb.........b.b.bb...b..bbebeeb.bb.bbe.eee.be
Disorder_S: 22222222233344445445554454544545565456565444332223332222223333333333332222322222222223322222322323 2
```

LRR

```
Dom:        _______8_____________________9_____________________10____________________11_____________________
No:         ........710.......720.......730.......740.......750.......760.......770.......780.......790.......800
            ---------|---------|---------|---------|---------|---------|---------|---------|---------|---------|
RPM1:       NLGCMTQLTRISLVMVRREHGRDLCDSLNKIKRIRFLSLTSIDEEEPLEIDDLIATASIEKLFLAGKLERVPSWFNTLQNLTYLGLRGSQLQENAILSIQ
PROF_sEc:   CCHHHHHHHHHHHHCCCCCCCCCHHHHHHHHHHHHHCCCCCCCCCCCCCCCCCCCCHHHHHHCCCCCCCCCCCCCCCCCCEEEEEECCCCCCCCHHHHH
Complexity: ........................................lllllllllll.....................................................
Access:     e-ee-ee-ee-e-ee-eeee-ee--e--ee-ee-ee---e--eeeee-e-ee-ee-ee-ee-e-e-e-ee--e--ee-ee-ee---ee-e-eeee-e--e
Access3:    .be.beeb..bbb.bb..e...ebbe.beeb.eb.bbbb.ebeee...eb........b.ebbe...b..b.ebbe.be.bbbbbb.bbeb.e.b.e.b.
Disorder_S: 3333333343334344444444433333332333333334443444444323222233222222323232222223232333333434333333333333
```

LRR

```
Dom:        ____12____________________13____________________14____________________15____________________
No:         ........810.......820.......830.......840.......850.......860.......870.......880.......890.......900
            ---------|---------|---------|---------|---------|---------|---------|---------|---------|---------|
RPM1:       TLPRLVWLSFYNAYMGPRLRFAQGFQNLKILEIVQMKHLTEVVIEDGAMFELQKLYVRACRGLEYVPRGIENLINLQELHLIHVSNQLVERIRGEGSVDR
PROF_sEc:   HHHHEEEEEECCCCCCCCCCCCCCCCCCCCEEEEECCCCCCCCCCCCCCCCCCCCEEEECCCCCCCCCHHHHHHHHHEEEEEECCCCCCCCCCCCCCCCCH
Complexity: ..........................................................................................................
Access:     e-ee-e-----e-eeeee-e--ee-ee-ee---ee-ee-ee-eeeeee-ee-ee---ee-ee-ee--ee-ee-ee-ee-e-ee-eee--ee-eeeeeee-
Access3:    .bb.bbbbbbb...b.e.b..be.be.b.bb.bb.be...ebbb....b.eb..bbb.bbe..e.bbebbeeb.eb..bbb....e.b.eebee.ee.e.
Disorder_S: 33222222221222221222222222221222223222222222212222222222223232222232222222233232332344445545575567667
```

```
Dom:        _____________________
No:         0.......910.......920.....
            ---------|---------|------
RPM1:       SRVKHIPAIKHYFRTDNGSFYVSLSS
PROF_sEc:   HHHHCCCCCHHHHCCCCCCCCCCCCC
Complexity: .........................
Access:     ee-ee-ee-e---e-ee-------ee
Access3:    ..be.be.b..b...eeeeb..ebee
Disorder_S: 554444443333333333333334665
```

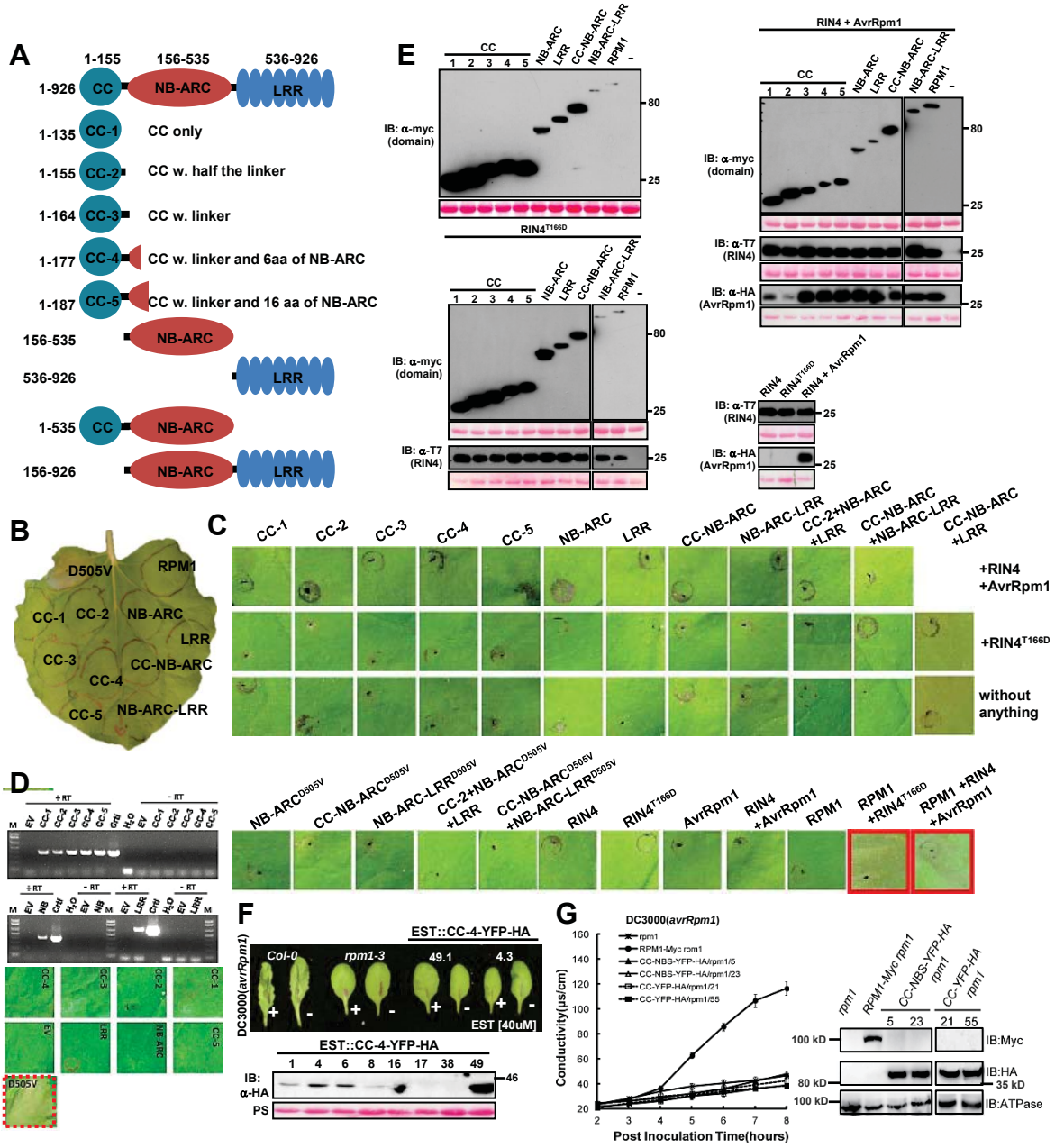

Fig. S2. Immune signaling is induced by activated full-length RPM1 only. **(*A*)** Schematic overview of full-length RPM1 and RPM1 fragments/domains used throughout this work. Fragment end- and start points were chosen based on secondary structure predictions and sequence comparisons with other plant NLR proteins. Numbers indicate amino acid start- and endpoints of indicated domains and fragments. **(*B*)** Lack of cell death induction by myc-epitope tagged RPM1 fragments and full-length RPM1 transiently expressed in *N. benthamiana*. MHD mutant RPM1^{D505V} was used as a positive control. **(*C*)** Lack of cell death induction in *N. benthamiana* by myc-epitope tagged RPM1 fragments transiently expressed alone (lower panel), together with RIN4^{T166D} (middle panel), RIN4 and dexamethasone inducible AvrRpm1-HA (upper panel). NB-ARC containing fragments/domains with the MHD motif mutation D505V and infiltration controls are shown in the very bottom panel. Images shown are representative of at least three biological replicates with at least 5 technical repeats each. Red boxes indicate positive controls for HR: full-length RPM1 with RIN4^{T166D} and full-length RPM1 together with RIN4 and AvrRpm1. **(*D*)** Epitope-tag does not influence lack of HR induction in transient expression in *N.benthamiana* by individual RPM1 fragments. Leaf images show representative results of expression of indicated non-tagged fragments individually; MHD motif mutant RPM1^{D505V} was used as a positive control for HR. DNA-gel pictures demonstrate transcription of indicated fragments *in planta*.

M, DNA-ladder; Crtl, positive control; EV, empty vector infiltration control; +RT and –RT, plus and minus reverse transcriptase, respectively. **(*E*)** Expression of myc-tagged RPM1 fragments and full-length protein, T7-tagged wild type and phosphomimetic RIN4 and HA-tagged AvrRpm1 from experiment shown in A. Proteins were extracted from transiently transformed *N. benthamiana* leaves 24 hours after infiltration (and 6 hours post induction in the case of dexamethasone inducible AvrRpm1-HA) and analyzed by immunoblotting with anti-myc, anti-T7 and anti-HA antibodies. Ponceau staining (PS) of the RuBisCO large subunit is a protein loading control. **(*F*)** Stable transgenic expression of YFP-HA tagged CC-4 fragment under the control of the estradiol inducible promoter in *pRIN4::T7-RIN4 rpm1-3 rps2-102c rin4* (*r1r2r4*) mutant Arabidopsis does not complement lack of AvrRpm1 recognition. Macroscopic HR in leaves of indicated genotypes 8 hours post infiltration of *Pto* DC3000(*avrRpm1*) and 24 hours post estradiol induction (upper panel). Immunoblot with anti-HA antibodies shows expression of 8 individual T3 lines expressing the YFP-HA tagged CC-4 fragment. Three plants each were pooled for protein extraction 6 hours after estradiol induction. Ponceau staining (PS) of the RuBisCO large subunit is a protein loading control. **(*G*)** Stable transgenic expression of YFP-HA tagged CC-2 and CC-NB-ARC fragments under the control of the 35S promoter in *rpm1-3* mutant Arabidopsis does not complement lack of AvrRpm1 recognition. Quantitative measurement of cell death (ion-leakage/conductivity) induced by activation of wild type RPM1 and indicated RPM1 fragments upon infiltration of *Pto* DC3000(*avrRpm1*) (left). Immunoblotting with anti-myc, anti-HA and anti-ATPase (for protein loading control) antibodies of indicated transgenic expressed proteins are shown (right).

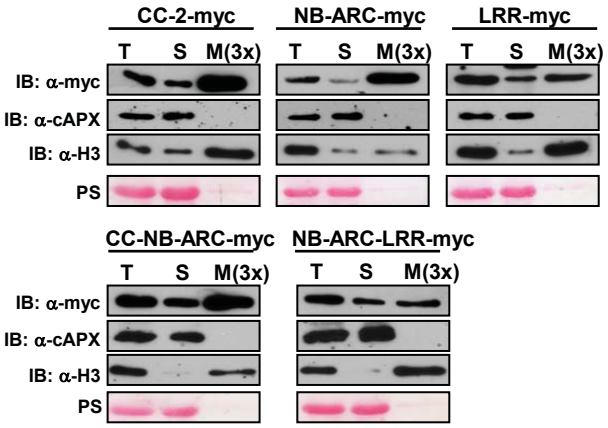

Fig. S3. Localization of RPM1 fragments and domains. Cell fractionation experiments show strong membrane localization of RPM1 CC-2, NB-ARC and the CC-NB-ARC fragments. myc-tagged 35S-driven RPM1 fragments were infiltrated into *N. benthamiana* leaves and tissue was harvested 48 hours post infiltration for cell-fractionation and western-blotting with anti-myc (RPM1), anti-APX (cytosol) and anti-H3 (Histone 3, membrane) antibodies. Ponceau S (PS) staining served as a protein loading control and an additional marker for the cytosolic fraction. T, total extract; S, soluble; M, microsomal fraction. M(3X) indicates 3 times enrichment relative to T or S.

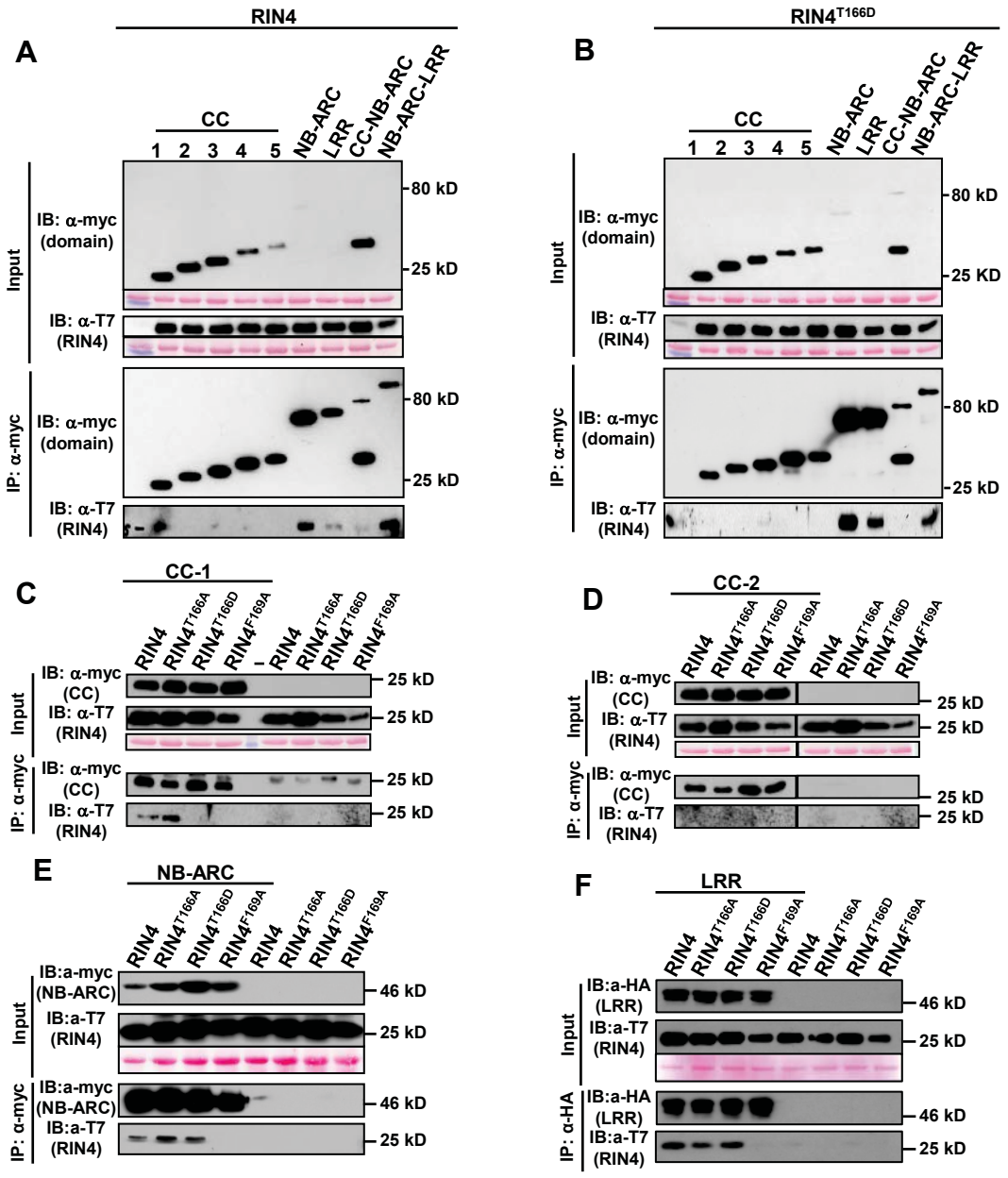

Fig. S4. *In planta* RPM1-RIN4 interaction is primarily mediated through the NB-ARC and LRR domains. **(*A*)** shows the interaction of the CC-1, NB-ARC, LRR and NB-ARC-LRR with wild type RIN4 and **(*B*)** the interaction of the NB-ARC, LRR and NB-ARC-LRR with RIN4^{T166D} transiently expressed in *N. benthamiana*. Note that the CC-NB-ARC fragment is not stable and gives rise to a truncated fragment as well – this was not consistently observed in all experiments. **(*C*-*F*)** Interaction analysis of transiently expressed CC-1 (*C*), CC-2 (*D*), NB-ARC (*E*) and LRR (*F*) domains with RIN4, RIN4^{T166A}, RIN4^{T166D} and RIN4^{F169A} by co-immunoprecipitation. RPM1 fragments were 35S promoter-driven and C-terminally myc-tagged, and N-terminal T7-tagged genomic RIN4 was expressed from its native promoter. Lysates were immunoprecipitated with anti-myc beads and then immunoblotted for both anti-myc and anti-T7 to assess input, immunoprecipitation and co-immunoprecipitation. Protein loading in input was assessed by Ponceau staining (PS). The RIN4^{F169A} mutant was used as a negative control for RPM1 fragment – RIN4 interaction. Note: bands present on the right in the anti-myc blot of the coIP fraction in (*C*) are non-specific, and the control experiment in (*D*) is from the same experiment as presented in (*C*), therefore the same control – RIN4 alleles w/o CC – is shown.

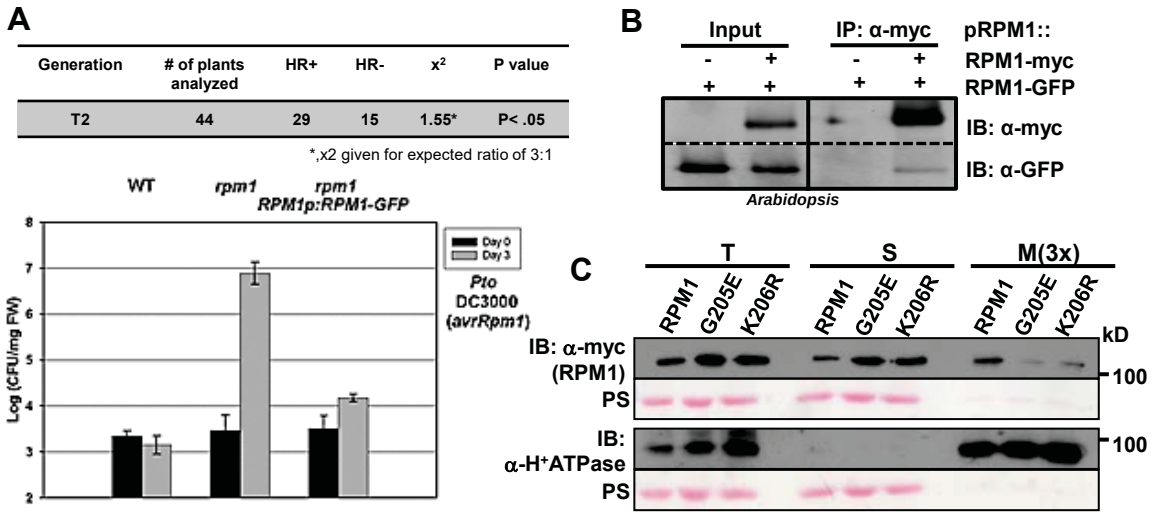

Fig. S5. RPM1 self-association and membrane localization is P-loop dependent. **(*A*)** Complementation of the *rpm1* mutant by the *pRPM1::RPM1-GFP* construct used to generate a double transgenic line. Table shows segregation of HR positive plants of one selected heterozygous T2 line. 44 plants were infiltrated with *Pto* DC3000(*avrRpm1*) (OD_{600}=0.1) and HR was scored 8 hours post infiltration. Bar-graph shows bacterial growth assay of indicated genotypes infiltrated with *Pto* DC3000(*avrRpm1*) (OD_{600}=0.0002) to assess complementation of growth restriction by *pRPM1::RPM1-GFP* in *rpm1-3*. WT, Col-0; *rpm1, rpm1-3; rpm1 pRPM1::RPM1-GFP*. **(*B*)** Self-association of RPM1-myc and RPM1-GFP in Arabidopsis. Stable transgenic expression in Arabidopsis was under the control of the *RPM1* promoter. Proteins were immunoprecipitated with anti-myc magnetic beads and then immunoblotted for both anti-myc and anti-GFP to assess input, immunoprecipitation and co-immunoprecipitation. **(*C*)** Cell fractionation analysis of wild type and P-loop alleles indicates decreased membrane localization of P-loop mutants. Indicated myc-tagged 35S-driven RPM1 constructs were infiltrated into *N. benthamiana* leaves and tissue was harvested for cell-fractionation and immunoblotting with anti-myc (RPM1) and anti-H^+ATPase (membrane) antibodies. Ponceau S (PS) staining is a protein loading control and marker for cytosolic fraction. T, total extract; S, soluble; M, microsomal fraction. M(3X) indicates 3 times enrichment relative to T or S.

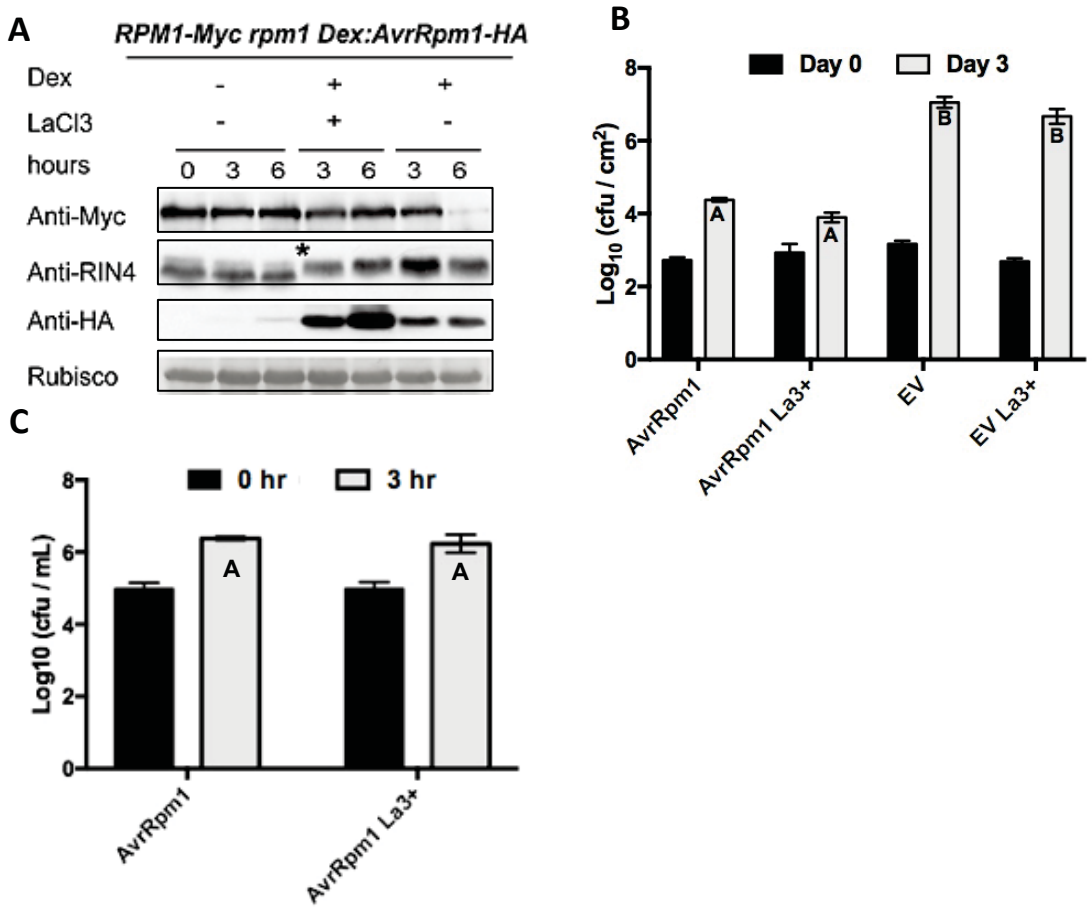

Fig. S6. Lanthanum ($LaCl_3$)-treatment does not affect RPM1-mediated disease resistance. **(*A*)** RPM1 protein accumulation upon $LaCl_3$-treatment. Disappearance of activated RPM1 was blocked by infiltration of 2mM $LaCl_3$ 30 minutes before dexamethasone (20uM) spraying to induce expression of the effector AvrRpm1-HA. AvrRpm1-inducing RIN4 modification was monitored with ~1 kDalton mobility shift by immunoblotting with anti-RIN4 (asterisk). AvrRpm1 expression was shown in immunoblot with anti-HA. Rubisco represents the protein loading control. **(*B*)** RPM1-mediated disease resistance in response to *Pto* DC3000(*avrRpm1*) in the presence of $LaCl_3$. 1.5mM $LaCl_3$ was added to the bacterial suspension ($1x10^5$ cfu/mL) and hand-infiltrated into leaves of Arabidopsis Col-0 plants. Bacterial growth of *Pto* DC3000(*avrRpm1*) and *Pto* DC3000(*EV*) was monitored at Day 0 and Day 3 with repeated application of 2mM $LaCl_3$ at 24 hour intervals. Student's *t*-test ($p < 0.01$) of bacterial growth in Day 0 or Day 3 was performed, respectively, and significance is indicated by letters in the bars. Error bars represent 2 x SE. **(*C*)** No effect of $LaCl_3$ on bacterial growth. The same amount of bacteria as used above ($1x10^5$ cfu/mL) was cultured in King's B media for 3 hours with and without 2mM $LaCl_3$. Statistical analysis was performed as in (*B*). Error bars represent 2 x SE and significance is indicated by letters in the bars.

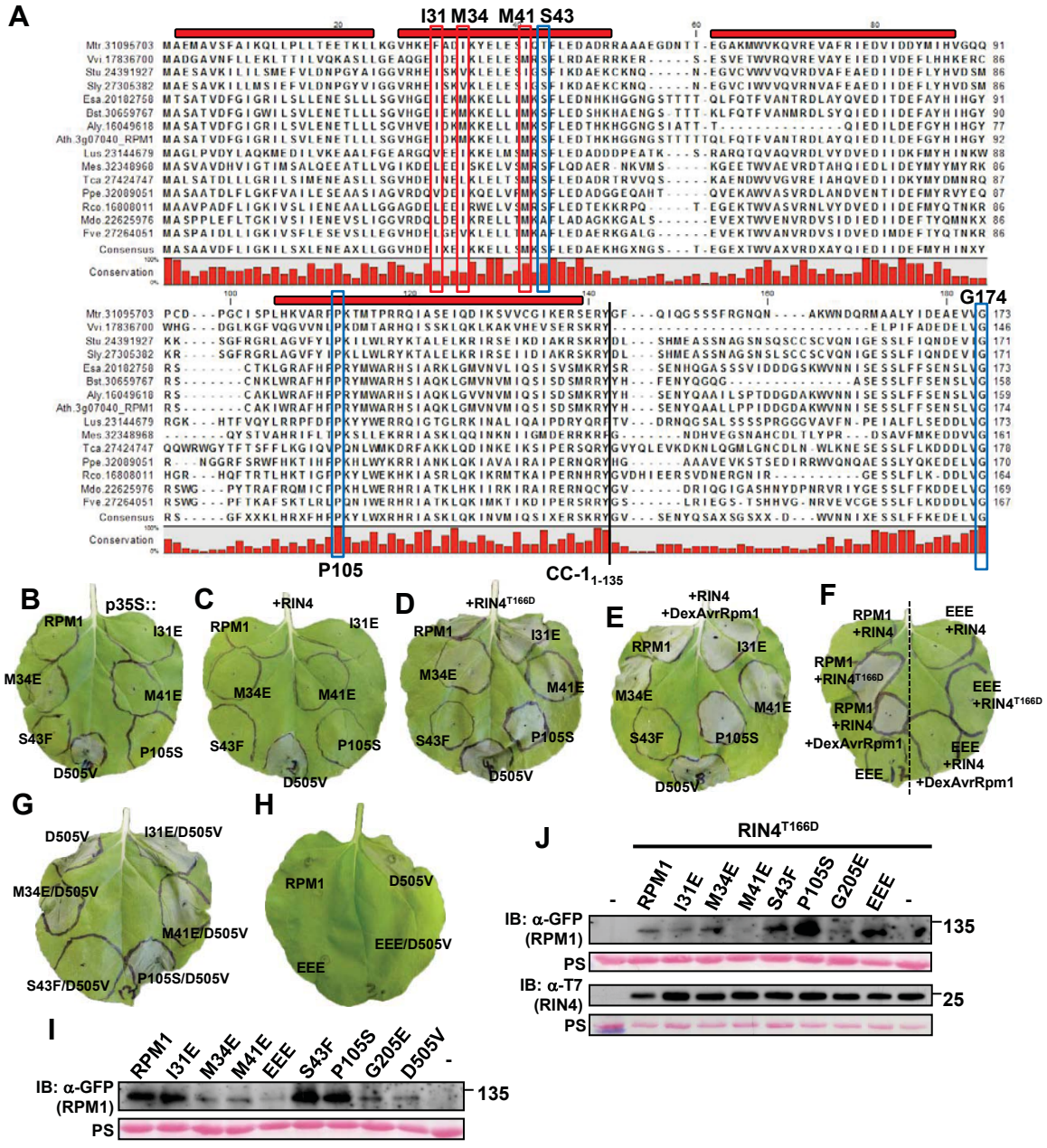

Fig. S7. Mutations in hydrophobic and conserved residues of the CC domain affect RPM1 function. **(*A*)** Protein sequence alignment and secondary structure prediction of full-length CC domain of Arabidopsis RPM1 and RPM1 orthologues. Red bars represent position of predicted alpha-helices for RPM1 CC domain. Positions of residues mutated and analyzed throughout this work are indicated and their conservation is highlighted by a red (hydrophobic residues) or blue (conserved residues) box. Transcript names are shown for each RPM1 orthologue in the specific plant species. Mtr, *Medicago truncatula*; Vvi, *Vites vinifera*; Stu, *Solanum tuberosum*; Sly, *Solanum lycopersicum*; Esa, *Eutrema salsugineum*; Bst, *Boechera stricta*; Aly, *Arabidopsis lyrata*; Ath, *Arabidopsis thaliana*; Lus, *Linum usitatissimun*; Mes, *Manihot esculenta*; Tca, *Theobroma cacao*; Ppe, *Prunus persicus*; Rco, *Ricinus communis*; Mdo, *Malus domesticus*; Fve, *Fragaria vesca*. **(*B-E*)** HR phenotypes induced by transient expression of the 35S promoter-driven CC domain mutants RPM1^{I31E}, RPM1^{M34E}, RPM1^{M41E}, RPM1^{S43F}.

and RPM1^{P105S} alone (*B*), together with RIN4 (*C*), phosphomimetic RIN4^{T166D} (*D*) or RIN4 and dexamethasone inducible AvrRpm1 (*E*). Wild type RPM1 and MHD motif mutant RPM1^{D505V} were used as controls. Images were taken 2 days post infiltration. Note that the mutations in the three hydrophobic residues I31, M34 and M34 as well as in P105 did not completely abolish RPM1 function when transiently over-expressed from the 35S promoter. **(*F*)** Loss of full activity of the RPM1$^{I31/M34/M41E}$ (EEE) triple mutant in the transient reconstruction assay in *N. benthamiana*. Left side of the leaf shows the control phenotypes with infiltrations of wild type RPM1 and the RPM1$^{I31/M34/M41E}$ (EEE) triple mutant alone and the right side of the leaf shows the experiment infiltrations with the triple mutant in co-expression with wild type RIN4 (upper right side), phosphomimetic RIN4^{T166D} (middle right side) and with wild type RIIN4 and dexamethasone inducible AvrRpm1 (lower right side). **(*G*)** HR phenotypes induced by *in cis* double mutants RPM1$^{I31E/D505V}$, RPM1$^{M34E/D505V}$, RPM1$^{M41E/D505V}$, RPM1$^{S43F/D505V}$ and RPM1$^{P105S/D505V}$. RPM1^{D505V} single mutant was used as a control for HR induction. Note that only the S43F mutation completely blocks RPM1^{D505V} auto-activity. **(*H*)** Complete block of RPM1^{D505V} auto-activity by RPM1$^{I31/M34/M41E}$ in the RPM1$^{I31/M34/M41E/D505V}$ *cis* quadruple mutant. All mutant RPM1 proteins in (*B-H*) were expressed from the 35S promoter. RIN4 and phosphomimetic RIN4^{T166D} were expressed from the RIN4 promoter. Images were taken 2 days post infiltration. **(*I, J*)** Expression of wild type and mutant RPM1 proteins shown in Fig. 3 *B* and *C*. Immunoblotting with anti-GFP and anti-T7 antibodies demonstrates accumulation of pRPM1::RPM1-eYFP (wild type and mutants) and phosphomimetic pRIN4::T7-RIN4^{T166D} proteins transiently expressed in *N. benthamiana*

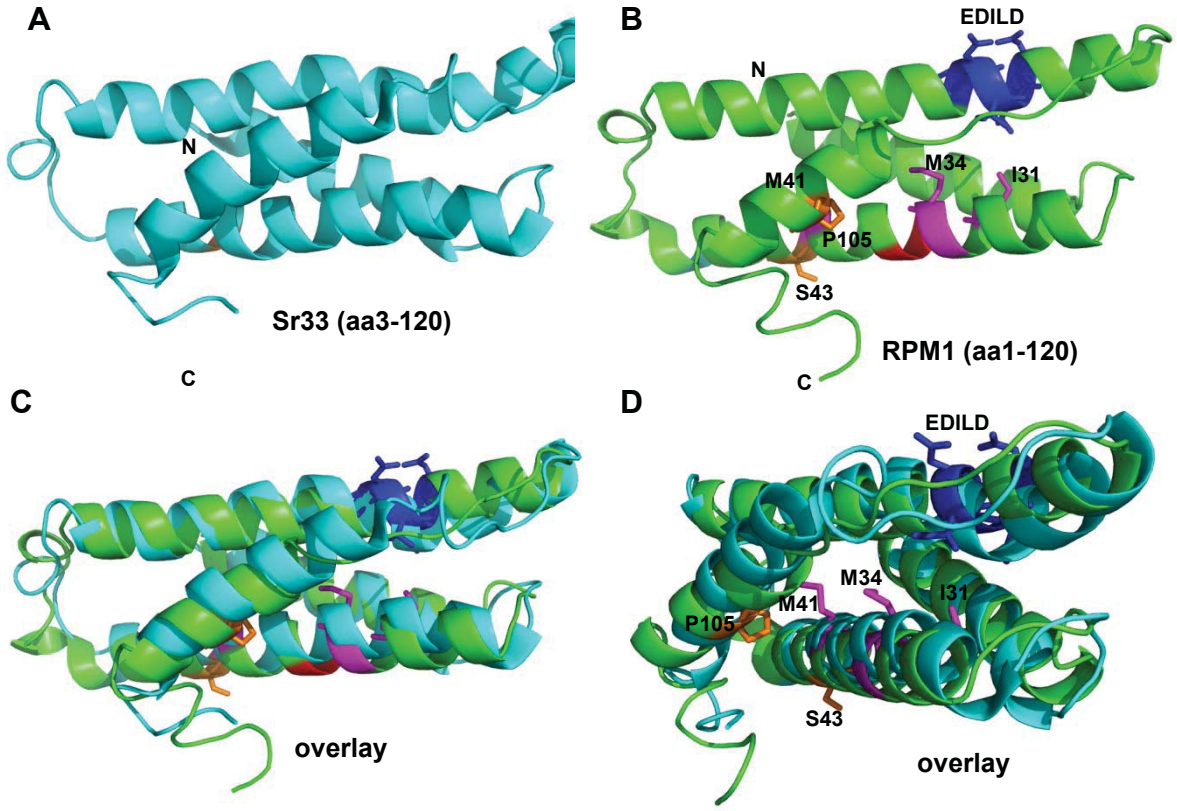

Fig. S8. Structural modelling of the RPM1 CC domain onto the Sr33 CC domain structure. **(*A*)** NMR structure of Sr33 CC domain (aa 3-120; PDB: 2NCG) as published by Casey et al. (10). N and C-termini are indicated. **(*B*)** Modelled structure of RPM1 CC domain (aa 1-120) indicates a very similar four-helical bundle conformation. Mutations used in this study are highlighted: hydrophobic residues I31, M34 and M41 in purple, conserved residues S43 and P105 in orange. The conserved EDVID motif (in RPM1 it is EDILD) is highlighted in blue. N and C-termini are indicated. **(*C, D*)** Overlay of the Sr33 (cyan) and RPM1 (green) CC domain structures, presented in a side view (*C*) and in a side view turned about 50 degrees to the viewer (*D*). Mutations in (*D*) are highlighted as in (*B*).

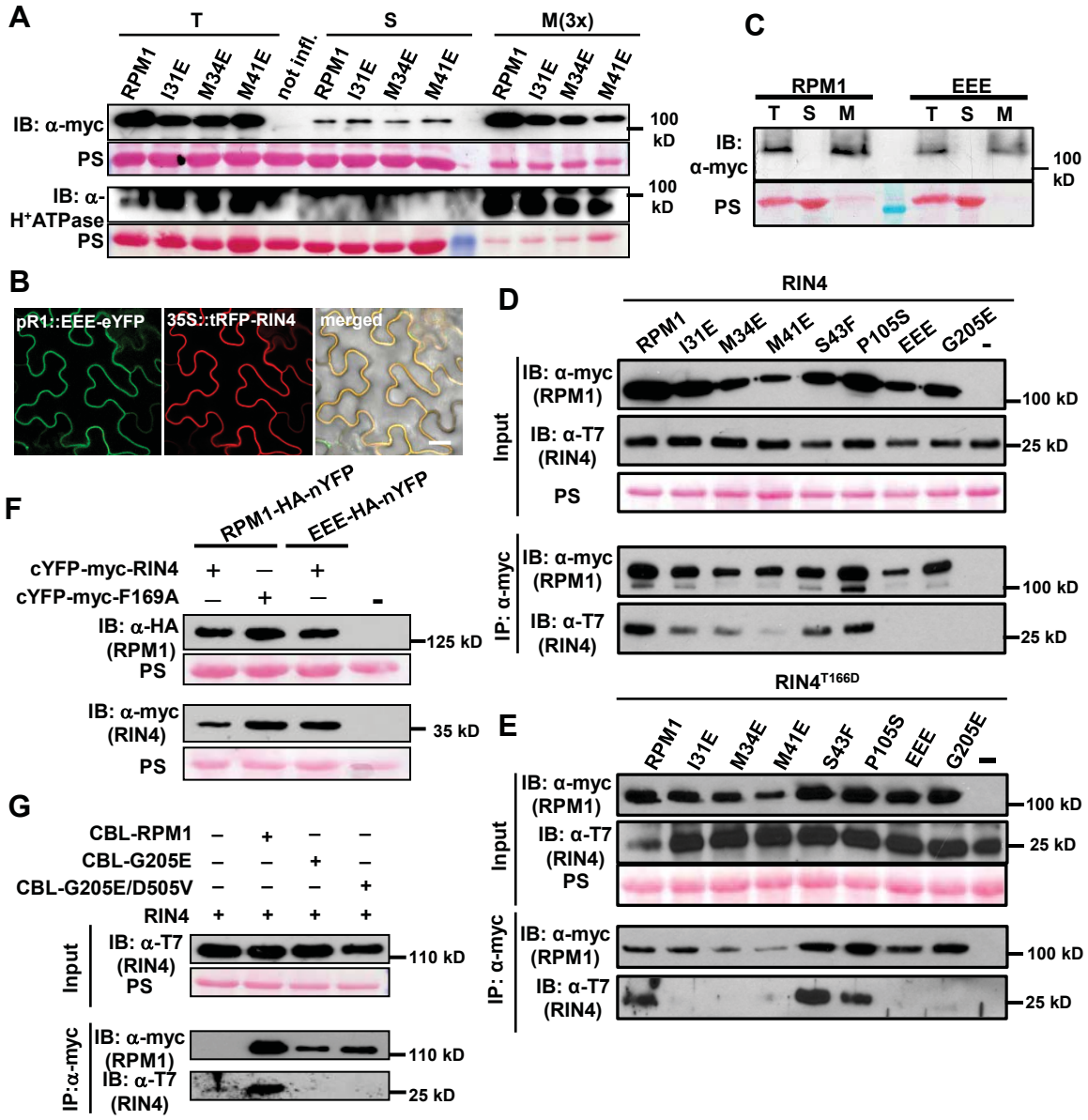

Fig. S9. RPM1-RIN4 interaction is dependent on the P-loop and the CC domain hydrophobic core. **(*A*)** The indicated myc-tagged 35S-driven RPM1 constructs were infiltrated into *N. benthamiana* leaves and tissue was harvested for cell-fractionation and western-blotting with anti-myc (RPM1), anti-H+ATPase (membrane) antibodies. Ponceau S (PS) staining served as protein loading control and marker for the cytosolic fraction. **(*B*)** Co-localization of RPM1$^{I31/M34/M41E}$-eYFP (pR1::EEE-eYFP) and tRFP-T7-RIN4 at the plasma membrane in *N. benthamiana* leaf-epidermal cells. pRPM1::RPM1$^{I31/M34/M41E}$-eYFP and 35S::tRFP-T7-RIN4 were co-infiltrated into 5 week old *N. benthamiana* leaves at and OD_{600} of 0.4 and 0.2, respectively and images were taken 48 hours post infiltration with a Leica LSM710 DUO confocal microscope. **(*C*)** Cell fractionation analysis of RPM1$^{I31/M34/M41E}$ demonstrates membrane localization. Indicated myc-tagged 35S-driven RPM1$^{I31/M34/M41E}$ and T7-RIN4 were infiltrated into *N. benthamiana* leaves and tissue was harvested for cell-fractionation and immunoblotting with anti-myc (RPM1) and anti-T7 (membrane) antibodies. Ponceau S (PS) staining served as protein loading control and marker for cytosolic fraction. T, total extract; S, soluble; M, microsomal fraction. M(3X) indicates

3 times enrichment relative to T or S. **(*D*)** Interaction of RPM1 with wild type RIN4 is P-loop dependent and also abolished by the triple CC domain mutation (EEE). T7-RIN4 was co-expressed with wild type or mutant myc-epitope tagged RPM1 in *N. benthamiana*. Proteins were immunoprecipitated with anti-myc magnetic beads and immunoblotted for both anti-myc and anti-T7 to assess input, immunoprecipitation and co-immunoprecipitation. **(*E*)** Interaction of phosphomimetic RIN4^{T166D} with RPM1 is strongly reduced by mutations in hydrophobic residues of the CC domain and mutation in the P-loop. Samples were processed as described in *D*. RPM1 and its derivatives were expressed from the 35S promoter, RIN4 and RIN4^{T166D} from its native promoter. Experiments were repeated two times with similar results. **(*F*)** Expression analysis of RPM1 and RIN4 derivatives sown in the BiFC experiment in Fig. 5H and I. Immunoblotting with anti-HA and anti-myc antibodies demonstrates accumulation of RPM1-HA-nYFP and cYFP-myc-RIN4. **(*G*)** Forced membrane-tethering of RPM1^{G205E} or RPM1$^{G205E/D505V}$ does not "rescue" loss of RIN4 interaction. Samples were processed as described in *D*. CBL-tagged RPM1 and its derivatives were expressed from the 35S promoter, RIN4 from its native promoter.

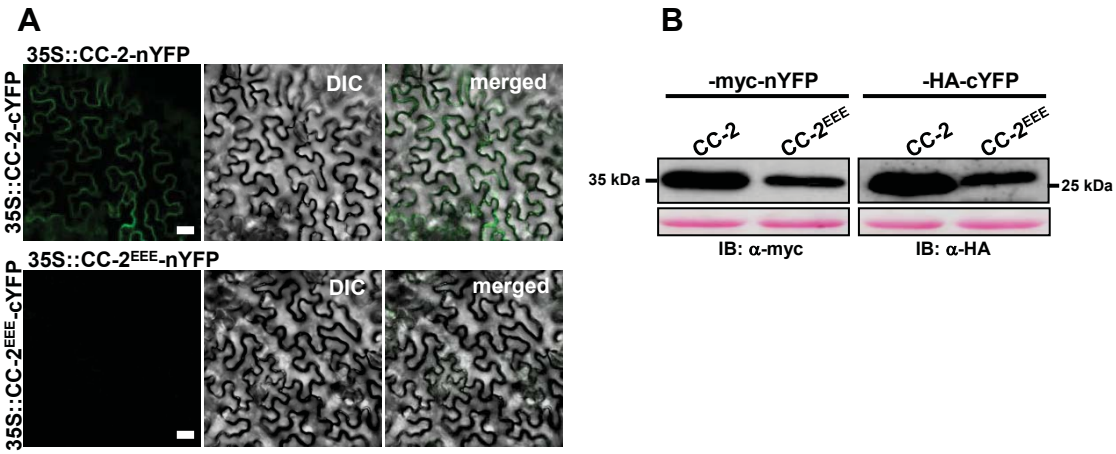

Fig. S10. CC-2 dimerization is blocked by mutations in hydrophobic residues. **(*A*)** Bimolecular fluorescence complementation (BiFC) by self-association of 35S promoter driven CC-2-cYFP, CC-2-nYFP, but not by CC-2^{EEE}-cYFP, CC-2^{EEE}-nYFP. Expression constructs were transiently expressed in *N. benthamiana* after infiltration of *Agrobacterium* containing indicated constructs at an OD_{600}=0.3. Images were taken 40 hours post infiltration. **(*B*)** Expression analysis of CC-2 and CC-2^{EEE} of the BiFC experiment in (*A*). Immunoblotting with anti-HA and anti-myc antibodies demonstrates accumulation of wildtype CC-2-HA-cYFP, CC-2-myc-nYFP and mutant CC-2^{EEE}-HA-cYFP, CC-2^{EEE}-myc-nYFP.

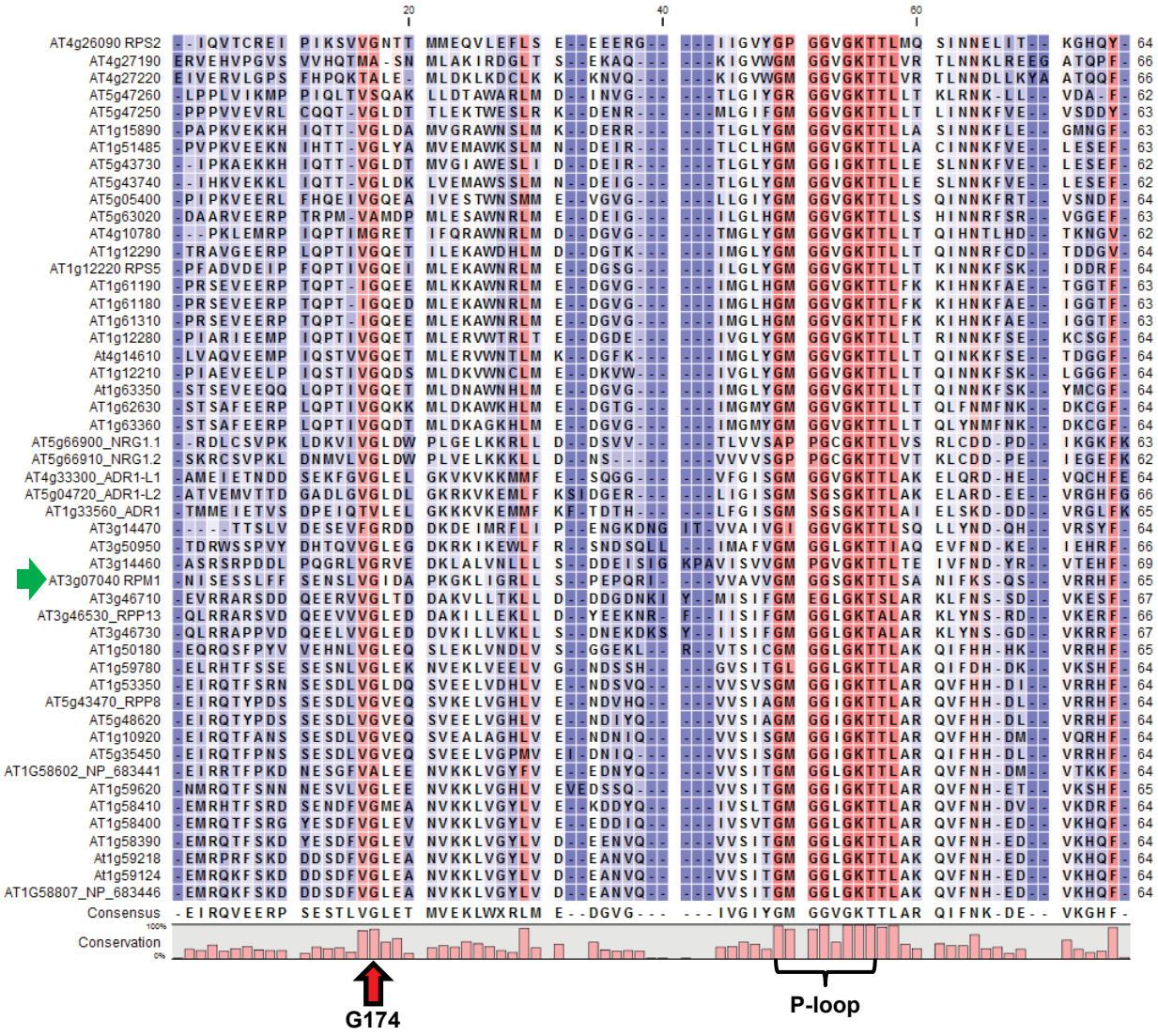

Fig. S11. Protein sequence alignment of Arabidopsis CNLs showing the conservation of Gly174. Sequences between amino acid 159-223 of RPM1 and other CNLs were aligned using the CLC Main Workbench MUSCLE alignment function. Color code indicates conservation of amino acids from low (blue) to high (red). Conserved Glycine residue and the P-loop are marked with a red arrow and a curly bracket, respectively. RPM1 sequence is highlighted by a green arrow.

Table S1. Documented self-association of full-length and/or domains of plant NLRs

NLR type	NLR	organism	self-association	epitope tags used [a]	P-loop dependent self-association	reference
CC/ CNL	RPM1	*Arabidopsis*	*yes (pre/post)*	*YFP/myc* [r]	*yes*	in this study
	RPS5	*Arabidopsis*	*yes (pre/post)*	*HA/myc* [r]	*n.a.*	(Ade et al., 2007)
	Rx	*potato*	*yes (pre/?)* [b]	*HA/myc*	*n.a.*	(Moffett et al., 2002) (Casey et al., 2016)
	Prf	*tomato*	*yes (pre)*	*HA/myc* [r]	*n.a.*	(Gutierrez et al., 2010)
	MLA10	*barley*	*yes (pre/?)* [b]	*CFP/HA*	*n.a.*	(Maekawa et al., 2011) (Casey et al., 2016) (Cesari et al., 2016)
	MLA1	*barley*	*yes (pre/post*)*	*myc/HA*	*n.a.*	(Maekawa et al., 2011)
	Rp-1D	*maize*	*yes*	*HA/GFP*	*n.a.*	(Wang et al., 2015)
	Sr33	*wheat*	*yes*	*CFP/ HA*	*n.a.*	(Casey et al., 2016) (Cesari et al., 2016)
	Sr50	*rye*	*yes*	*CFP/HA*	*n.a.*	(Casey et al., 2016) (Cesari et al., 2016)
	RGA4/RGA5	*rice*	*yes (pre/post)*	*GFP/HA*	*n.a.*	(Césari et al., 2014)
TIR/ TNL	$RPP1_{Nd}$	*Arabidopsis*	*yes (post*)*	*FLAG/HA*	*yes*	(Schreiber et al., 2016; Zhang et al., 2017)
	Dm2/ DM1d	*Arabidopsis*	*yes (pre)*	*HA/myc*	*yes* [d]	(Tran et al., 2017)
	SNC1	*Arabidopsis*	*yes (pre/post?)*	*FLAG/HA FLAG/aSNC1 GFP/aSNC1*	*n.a.*	(Xu et al., 2014; Zhang et al., 2017)
	RPS4/ RRS1	*Arabidopsis*	*yes (pre/post)* [c]	*FLAG/HA* [r]	*no* [d]	(Sohn et al., 2014) (Williams et al., 2014)
	RBA1	*Arabidopsis*	*yes (pre/post)*	*myc/HA* [r]	-	(Nishimura et al., 2017 PNAS)
	N	*tobacco*	*yes (post*)*	*HA/myc*	*yes*	(Mestre and Baulcombe, 2006)
	L6/L7	*flax*	*yes* [b]	*only in yeast and in vitro*	*n.a.*	(Bernoux et al., 2016; Zhang et al., 2017) (Bernoux et al., 2011)

*n.a.= not analyzed; [r]= IP also done reciprocally; *= self-association in presence of recognized effector; [a]= tag used for pulldown is mentioned first; [b]= self-association shown only for domain(s); [c]= association also shown for heterodimer; [d]= tested only for heterodimer formation*

Table S2. Primer sequences used in this study

Primer	Sequence (5' to 3')	Comment
FEK_1	CACCATGGCTTCGGCTACTGTTGATTTTGG	RPM1 start + pENTR (CACC) sequence 5'
FEK_2	GTACCTTTTCATGGAATCAGAAATGGATTGAATC	RPM1 CC-1 backward primer
FEK_3	AGATGACTCACTGATGTTGTTCACCCACTTTGC	RPM1 CC-3 backward primer
FEK_4	TGCATCAATCCCTACAAGACTATTTTCACTAAAG	RPM1 CC-4 backward primer
FEK_5	TAGAAGCCGTCCGATGAGCTTTCCCTTGGGTGC	RPM1 CC-5 backward primer
FEK_83	ctaGTACCTTTTCATGGAATCAGAAATGGATTGAATC	cloning CC 1 with STOP codon
FEK_87	ctaCTTTGCATCGCCATCATCAATAGG	cloning CC-2 with STOP codon
FEK_84	ctaAGATGACTCACTGATGTTGTTCACCCACTTTGC	cloning CC-3 with STOP codon
FEK_85	ctaTGCATCAATCCCTACAAGACTATTTTCACTAAAG	cloning CC-4 with STOP codon
FEK_86	ctaTAGAAGCCGTCCGATGAGCTTTCCCTTGGGTGC	cloning CC-5 with STOP codon
FEK_88	ctaAGTTTCTGCAGCATCATCACCATC	cloning NB with STOP
FEK_89	CTAAGATGAGAGGCTCACATAGAAAGAGC	RPM1 backward plus stop
FEK_205	GGGGACAAGTTTGTACAAAAAAGCAGGCTtaATGGCACGTTCGAATGTACC	adding attB1 site to RIN4 forward for cDNA
FEK_206	GGGGACAACTTTGTATAGAAAAGTTGGGTgTCATTTTCCTCCAAAGCCAA	adding attB4 site to RIN4 reverse
FEK_207	GGGGACAACTTTGTATAATAAAGTTGtaATGGCTTCGGCTACTGTTGA	adding attB3 site to RPM1 forward
FEK_208	GGGGACCACTTTGTACAAGAAAGCTGGGTtAGATGAGAGGCTCACATAGA	adding attB2 site to RPM1 reverse
FEK_209	GGGGACAAGTTTGTACAAAAAAGCAGGCTtaATGGCAGTAAGTGTTTTCTTTCCTTCTTTCC	adding attB1 site to RIN4 forward for genomic fragment
FEK_592	GGGGACAAGTTTGTACAAAAAAGCAGGCTtaATGGCTTCGGCTACTGTTGATTTTGG	attB1 site forward RPM1
FEK_593	GGGGACAACTTTGTATAGAAAAGTTGGGTgAGATGAGAGGCTCACATAGAAAGAGC	attB4 site reward RPM1
I31E forward	GTCCATGGTGAGGAGGATAAAATGAAGAAG	site-directed mutagenesis primer mutating I31 to E in RPM1
I31E backward	CTTCTTCATTTTATCCTCCTCACCATGGAC	site-directed mutagenesis primer mutating I31 to E in RPM1
M34E forward	GTGAGATTGATAAAGAGAAGAAGGAGTTG	site-directed mutagenesis primer mutating M34 to E in RPM1
M34E backward	CAACTCCTTCTTCTCTTTATCAATCTCAC	site-directed mutagenesis primer mutating M34 to E in RPM1
M41E forward	GGAGTTGCTGATCgaGAAGTCCTTTCTTG	site-directed mutagenesis primer mutating M41 to E in RPM1
M41E backward	CAAGAAAGGACTTCtcGATCAGCAACTCC	site-directed mutagenesis primer mutating M41 to E in RPM1
FEK_50	CATGGTGAGgagGATAAAgaGAAGAAGGAGTTGCTGATCgaGAAGTCCTTTCTT	site-directed mutagenesis primer for making RPM1 EEE triple mutant version
FEK_51	AAGAAAGGACTTCtcGATCAGCAACTCCTTCTTctcTTTATCctcCTCACCATG	site-directed mutagenesis primer for making RPM1 EEE triple mutant version
FEK_96	gatcTcTAgAATGAAACTATGATCGAGGTTGGTAAC	forward primer for amplifying the full RPM1 promotor region with XbaI sites
FEK_54	gatcTcTAgACTTCCTCAGAGTCTCGCTTGAACC	reward for cloning of RPM1promotor in front of gateway cassette in XbaI site